Th LHR4 05

Anisotropic Velocity Model Calibration in Surface Monitoring Using Microseismic Events - A Case Study

T.S. Becker* (ETH Zurich), I.A. Vera Rodriguez (Schlumberger Gould Research), I. Bradford (Schlumberger Gould Research), A. Gendrin (Schlumberger Gould Research) & J.O.A. Robertsson (ETH Zurich)

SUMMARY

This abstract presents a case study where an anisotropic velocity model for surface microseismic monitoring is obtained from travel time inversion using P- and SV-wave arrivals of microseismic events that are observable on the surface records. Additionally, we correct for statics using cross-correlation of the P-wave arrivals of the same events. The calibration of the velocity model proves robust to uncertainties in the locations of the reference events. The comparison to event locations derived with an isotropic velocity model results in negligible differences in the epicentre and comparable depths of events. Finally, the application of static corrections shifts the event locations while increasing the maximum stacked energy, suggesting improvement in location accuracy. The findings emphasize the relative importance of near-surface effects over the importance of anisotropy and heterogeneity for this particular case study.

Introduction

The successful outcome of event localization and the derivation of source mechanisms from hydraulic fracture monitoring (HFM) data rely on a robust velocity model (e.g., Warpinski *et al*., 2009). For downhole monitoring, the wave arrivals of perforation shots with known source positions are often used to constrain the parameters of a calibrated velocity model (e.g., Le Calvez *et al*., 2013). In the case of HFM with surface arrays, the increased source-receiver distance and higher levels of noise often prohibit the use of perforation shots for calibration, because they become more difficult to detect. Using a case study, this abstract exemplifies a workflow that overcomes this limitation through the use of strong microseismic events with wave arrivals that are observable in a set of surface monitoring records. The locations of the selected calibration events are estimated with an initial homogeneous and isotropic velocity model. Numerical experiments evaluate the robustness of the calibrated model parameters to event location errors. The P-wave arrivals of the same events are also used to estimate static corrections based on cross-correlation. Location results obtained using an isotropic model, the anisotropic model calibrated in this work, and the anisotropic model incorporating static corrections are analysed in an attempt to identify which scenario provides the most reliable event locations.

Construction of the Initial Velocity Model

The monitoring array of the case study consists of 10 surface lines with 1082 vertical-component geophones. Available well logs of vertical compressional velocity (α_0), vertical shear velocity (β_0) and density (ρ) display small property contrasts along most of their vertical extent. Backus-averaging of the logs (Backus, 1962) resulted in an equivalent medium composed of 7 homogeneous layers (Figure 1). Most of the significant rock-property contrasts in the blocked model are limited to a region of about 50 m above the reservoir. Between 1720 m and 1940 m the blocked model consists of a single layer. No log readings were available from the surface to 1720 m. Consequently, the uppermost layer of the blocked model was extended up to the surface. This assumption is in line with previous processing results of the surface records, where extension of the velocity model was achieved based on the moveout correction of the arrivals of observed microseismic events. The average elevation of the study area was assigned to all receivers due to the lack of information on the vertical receiver coordinates. Given a maximum variation in elevation between receivers of about 100 m, it was anticipated that the small errors in travel time introduced by the change of datum could be compensated for by static corrections. Finally, an available seismic interpretation also suggested a subtle dip of the reservoir of about 1° towards east-northeast (60°) in the monitored region. This was incorporated into the model via a rotation of the layers in the dip direction.

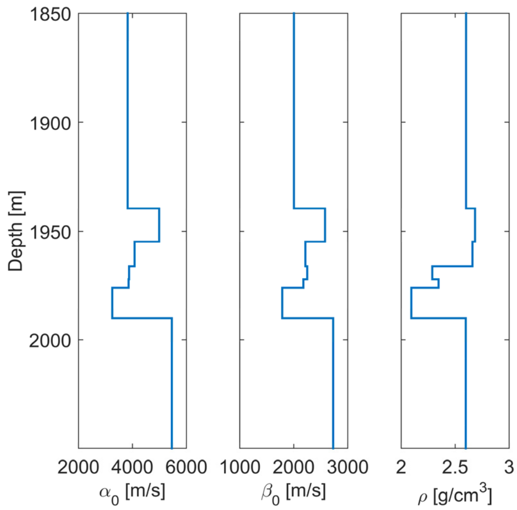

Figure 1 *Initial blocked velocity and density logs consisting of seven homogeneous layers.*

Velocity Model Calibration

The P- and S_V-wave arrivals of five strong microseismic events were manually picked on the surface traces. The locations of these events were estimated in a combined Bayesian inversion and migration approach (Coalescence Microseismic Mapping; Drew *et al*., 2005) using an available homogenous, isotropic velocity model (Figure 2). Considering that previous work demonstrated robustness in the estimation of the epicentre of microseismic events to errors in the velocity model using surface monitoring arrays (e.g., Eisner *et al*., 2009), and that the estimated depth of the selected events falls within the reservoir region, it was assumed that the locations of the events were well constrained by the isotropic model. Nevertheless, further numerical tests, described in more detail later, were performed to assess the sensitivity of the calibrated velocity model to individual reference events and to errors in the location of these events. In both cases, a non-linear inversion approach was used to estimate ε and δ (Thomsen, 1986) and updates for α_0 and β_0 of the first model layer by minimizing the misfit between the observed travel times and the travel times predicted using ray tracing (Mizuno *et al*., 2010). The blocked well logs were used to initialize the inversion. This resulted in a tilted transverse isotropic (TTI) medium with a single axis of symmetry, which is commonly associated with layered, clay-rich strata (Tsvankin, 2001).

Table 1 *Parameters of the homogeneous, anisotropic velocity model (first row) and mean and standard deviation from ten inversions using perturbed reference event locations (second and third row).*

	α_0 [m/s]	β_0 [m/s]	ε	δ
Model	3633	2142	0.310	0.160
mean	3640	2141	0.307	0.156
σ	6	8	0.005	0.010

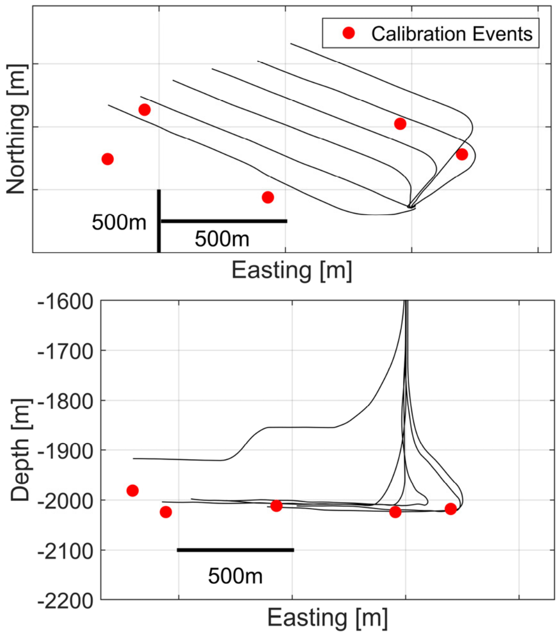

Figure 2 *Map (top) and section (bottom) views of the estimated locations of the five events used for model calibration and static corrections. For the bottom plot, the view is towards the north.*

In a first analysis, the robustness of the model and its sensitivity to individual events was tested by repeating the calibration of the blocked model six times—once using all five events and five times iteratively omitting one of the events. The same procedure was applied to a homogeneous model with initial values based only on the first layer of the blocked model. The calibration of both models led to similar values for α_0, β_0, and ε, with relative differences below 3% between the homogeneous model and the weighted average of the layered model. Relative differences in δ reached up to 85%. However, the layered model showed slightly larger standard deviations for the anisotropy parameters as well as the shear velocity, indicating a larger sensitivity with respect to individual events used for the calibration. The analysis suggests that the increased complexity of the layered model is not beneficial for microseismic event localization in this case study. In a second analysis, the sensitivity of the homogeneous model to errors in source locations of the reference events was tested. Event locations were perturbed with random errors of up to 50 m before repeating the calibration. Ten iterations with erroneous source positions were carried out. Table 1 presents the resulting model parameters as well as the results of the sensitivity analysis. All model parameters exhibit small standard deviations (σ), suggesting robustness with respect to errors in the locations of the microseismic events used for calibration.

Static Corrections

To account for velocity heterogeneities and the effects of topography, static corrections were applied. Statics were estimated through a data-driven approach that relies on cross-correlation of arrivals of the same events that were used for the model calibration. The P-wave arrivals of these events were moveout-corrected by subtracting travel times predicted via ray tracing with the calibrated homogeneous, anisotropic model. For each of the five events, a master trace with a clear P-wave arrival was cross-correlated with the remaining traces. The lag of the maximum positive correlation peak was the required static correction per receiver to align the arrival (Figure 3). Although the events are distributed across the study area and originate from different hydraulic treatment stages, time shifts for all events closely follow the mean value for most receivers. This supports the conclusion that static corrections are consistent across the monitored region and allowed using the mean values across the entire study area.

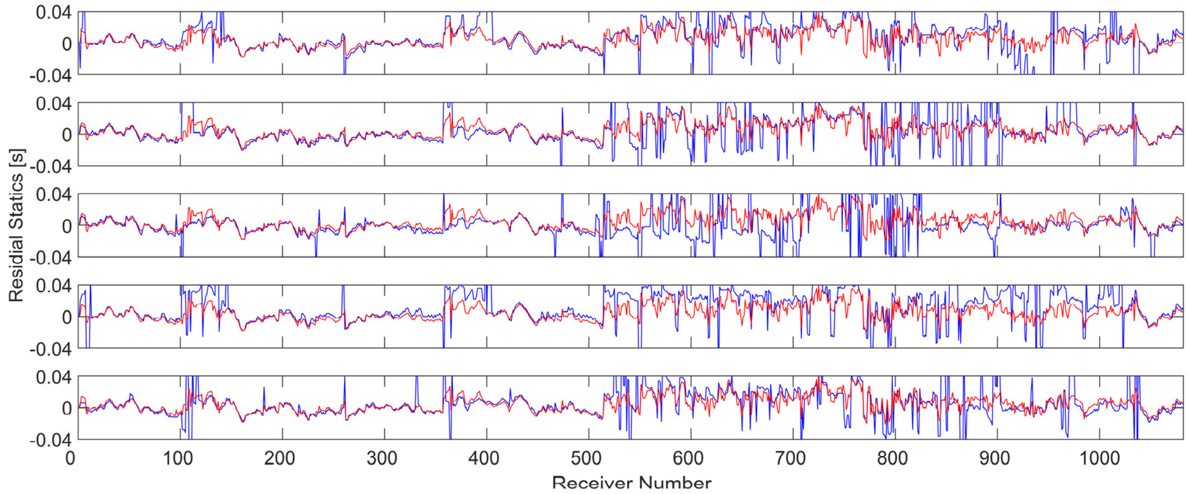

Figure 3 *Calculated correlation lags (i.e., static corrections) for all 1082 receivers for the five reference events (blue) and mean correlation lag (red) ignoring lags above/below +/- 40 ms.*

Localization Results

The calibrated velocity model and residual statics were used to process 15 hydraulic treatment stages. A comparison of location results using the homogeneous, isotropic model versus the homogeneous, anisotropic model without residual statics shows no significant difference in terms of location (Figure 4) and magnitude of stacked energy per event. The incorporation of residual statics, on the other hand, introduces visible changes in the event locations (Figure 4) and an increase in the magnitude of stacked energy in each located event. The increase in stacked energy reflects a better approximation of the moveout of observed arrivals by the anisotropic model and statics.

Conclusion

We derived a layered and a homogeneous, anisotropic velocity model calibrated from P- and S_V-wave arrivals of microseismic events recorded at the surface. The calibrated homogeneous model displayed more consistency in model parameters when the calibration was repeated, omitting sequentially one of the reference events. The well logs only displayed significant velocity contrasts in an interval of about 50 m above the reservoir (3% of the travel path from the reservoir to the surface), while the uppermost 220 m of the logs exhibit very little variation in velocity. For this reason, and since the extension of the homogeneous velocity model to the surface produced robust moveout corrections (not shown in this work), the homogeneous assumption seems justifiable in this scenario. The calibration of the homogeneous model proved also robust to errors in the assumed location of the reference events. The comparison between locations obtained with the anisotropic model and an isotropic model shows negligible differences in epicentres and comparable depths of events. The first observation is consistent with earlier work that reported robust epicentres of events located from surface data with respect to errors in the velocity model. Applying static corrections shifts and increases the maximum stacked energy (the predicted event location), suggesting improved event locations. These observations suggest that for this case study, near-surface effects are more important to account for to improve locations than anisotropy effects. Further investigations of potential advantages of the anisotropic, elastic velocity model are underway, for example, including shear waves in the localization process to improve depth resolution. Moreover, the estimation of fracture planes relies on removing the elastic parameters from inverted moment tensors.

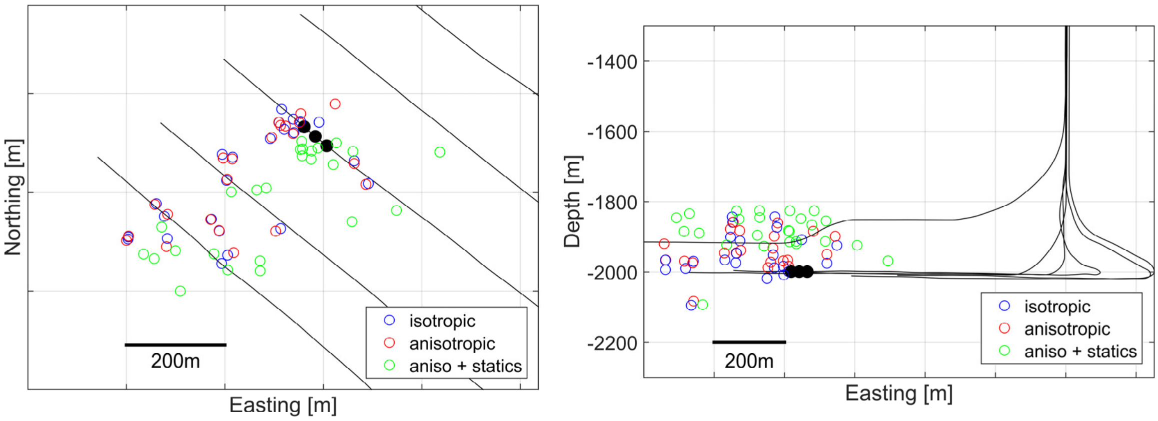

Figure 4 *Map (left) and section (right) views of filtered events for one stage localized with the surface array using the isotropic model (blue), the anisotropic model (red) and the anisotropic model with static corrections (green). Perforation shots are denoted with black circles and well trajectories are shown with black lines. For the plot on the right the view is towards north.*

Acknowledgments

We thank Schlumberger for allowing publication of this work. Furthermore, we thank Dirk-Jan van Manen in ETH Zurich, and three other reviewers within Schlumberger for revision of the abstract.

References

Backus, G.E. [1962] Longwave elastic anisotropy produced by horizontal layering. *Journal of Geophysical Research*, **67**(11), 4427–4440.

Drew, J., Leslie, D., Armstrong, P. and Michaud, G. [2005] Automated microseismic event detection and location by continuous spatial mapping. *SPE Annual Technical Conference and Exhibition*, SPE-95513-MS.

Eisner, L., Duncan, P., Heigl, W. and Keller, W. [2009] Uncertainties in passive seismic monitoring. *The Leading Edge*, **28**(6), 648-655.

Le Calvez, J., Williams, M. and Couch, J. [2013] Tool and Velocity Model Calibration for Downhole-Based Hydraulic Fracture Monitoring of Induced Microseismicity. *SEG Annual Meeting*, SEG-2013-0212.

Mizuno, T., Leaney, S. and Michaud, G. [2010] Anisotropic velocity model inversion for imaging the microseismic cloud. *72nd EAGE Conference & Exhibition,* Extended Abstracts, F014.

Thomsen, L. [1986] Weak elastic anisotropy. *Geophysics*, **51**(10), 1954-1966.

Tsvankin, I.D. [2001] Seismic signatures and analysis of reflection data in anisotropic media. In: Helbig, K. and Treitel, S. (Eds.) *Handbook of Geophysical Exploration*. Pergamon, Amsterdam and New York.

Warpinski, N.R., Waltman, C.K., Du, J. and Ma, Q. [2009] Anisotropy effects in microseismic monitoring. *SPE Annual Technical Conference and Exhibition,* SPE-124208-MS.